SUPPLEMENTARY DATA

Mre11 ATLD17/18 mutation retains Tel1/ATM activity but blocks DNA double-strand break repair

Oliver Limbo[1,5], Davide Moiani[1,2,5], Aryandi Kertokalio[3], Claire Wyman[3], John A. Tainer[1,2,4*], Paul Russell[1*]

[1]Department of Molecular Biology, [2]Skaggs Institute for Chemical Biology, The Scripps Research Institute, 10550 North Torrey Pines Rd., La Jolla, CA 92037, USA
[3]Department of Radiation Oncology, Department of Cell Biology and Genetics, Erasmus University Medical Center, PO Box 2040, 3000 CA, Rotterdam, The Netherlands
[4]Life Sciences Division, Department of Molecular Biology, Lawrence Berkeley National Laboratory, Berkeley, CA 94720, USA

*To whom correspondence should be addressed. Tel: (858) 784-8273; Fax: (858) 784-8273; E-mail: prussell@scripps.edu. Correspondence may also be addressed to: Tel: (858) 784-8119; Fax: (858) 784-2277; E-mail: jat@scripps.edu

[5]The authors wish it to be known that, in their opinion, the first two authors should be regarded as joint First Authors

Table S1: X-Ray data collection phasing, and refinement statistics

Data Collection	
Molecule	pfMre11 L204R
Beamline	ALS-BL12.3.1
Space group	P 1 21 1
Cell dimensions	a (Å) 68.03 b (Å) 70.18 c (Å) 81.48
Wavelength (Å)	1.1158
Resolution range (Å)	45-2.30
Unique reflections	30428
Completeness (%) (last shell)	99.0 (90.2)
Rsym (last shell)	0.100 (0.404)
I/Sigma (last shell)	13.8 (3.3)
Refinement Statistics	
Resolution range (Å)	50-2.30
R_{work}/R_{free} (%)	22.3/27.6
Refined atoms	5500
R. m. s. Bonds (Å) / Angles (°)	0.019 / 1.875

Table S2. *S. pombe* strains used in this study

Strain	Genotype (all *leu1-32 ura4-D18*)	Source
PR109	*h⁻*	Lab stock
PR110	*h⁺*	Lab stock
OL4177	*h⁻ mre11::kanMX4*	Williams 2008
OL4399	*h⁺ mre11::kanMX4*	Limbo 2007
OL5062	*h⁺ mre11::natMX6*	This study
OL5063	*h⁻ mre11-13MYC:kanMX6*	This study
OL5064	*h⁺ mre11-13MYC:kanMX6*	This study
OL5065	*h⁻ mre11-W248R-13MYC:kanMX6*	This study
OL5066	*h⁺ mre11-W248R-13MYC:kanMX6*	This study
yFS658	*h⁺ mre11-N122S-13MYC:natMX6*	Porter-Goff 2009
yFS659	*h⁺ mre11-W215C-13MYC:natMX6*	Porter-Goff 2009
JW4171	*h⁻ mre11-H134S-13MYC:kanMX6*	Williams 2008
OL5067	*h⁺ mre11-H134S-13MYC:kanMX6*	This study
OL5068	*h⁺ mre11-H134S-13MYC:hphMX6*	This study
SC4800	*h⁻ rad22-RFP:natMX6*	This study
OL5069	*h⁻ mre11::kanMX4 rad22-RFP:natMX6*	This study
OL5070	*h⁻ mre11-N122S-13MYC:natMX6 rad22-RFP:natMX6*	This study
OL5071	*h⁻ mre11-W215C-13MYC:natMX6 rad22-RFP:natMX6*	This study
OL5072	*h⁻ mre11-W248R-13MYC:kanMX6 rad22-RFP:natMX6*	This study
OL5073	*h⁻ mre11-H134S-13MYC:kanMX6 rad22-RFP:natMX6*	This study
OL5074	*h⁺ mre11-13MYC:kanMX6 TAP-rad50:kanMX6 nbs1-5FLAG:kanMX6*	This study
OL5075	*h⁺ mre11::natMX6 TAP-rad50:kanMX6 nbs1-5FLAG:kanMX6*	This study
OL5076	*h⁺ mre11-W248R-13MYC:kanMX6 TAP-rad50:kanMX6 nbs1-5FLAG:kanMX6*	This study
OL5077	*h⁺ mre11-N122S-13MYC:natMX6 TAP-rad50:kanMX6 nbs1-5FLAG:kanMX6*	This study
OL5078	*h⁺ mre11-W215C-13MYC:natMX6 TAP-rad50:kanMX6 nbs1-5FLAG:kanMX6*	This study
OL5079	*h⁺ mre11-H134S-13MYC:kanMX6 TAP-rad50:kanMX6 nbs1-5FLAG:kanMX6*	This study
YY4138	*h⁺ arg3::HOsite:kanMX4 ars1::nmt41-HO endonuclease:ampR:his3⁺:ars1⁺ his3-D1*	Limbo 2007
YY5080	*h⁺ mre11-13MYC:kanMX6 arg3::HOsite:kanMX4 ars1::nmt41-HO endonuclease:ampR:his3⁺:ars1⁺ his3-D1*	This study
OL5081	*h⁺ mre11-W248R-13MYC:kanMX6 arg3::HOsite:kanMX4 ars1:nmt41-HO endonuclease:ampR:his3⁺:ars1⁺ his3-D1*	This study
LLD3427	*h⁻ chk1-9MYC-2HA6his:ura4⁺*	Du 2004
OL4873	*h⁻ mre11::kanMX4 chk1-9MYC-2HA6his:ura4⁺*	Limbo 2011
OL5082	*h⁻ mre11-N122S-13MYC:natMX6 chk1-9MYC-2HA6his:ura4⁺*	This study
OL5083	*h⁻ mre11-W215C-13MYC:natMX6 chk1-9MYC-2HA6his:ura4⁺*	This study
OL5084	*h⁻ mre11-W248R-13MYC:kanMX6 chk1-9MYC-2HA6his:ura4⁺*	This study
OL5085	*h⁺ mre11-W248R-13MYC:kanMX6 chk1-9MYC-2HA6his:ura4⁺*	This study
OL4874	*h⁻ mre11-H134S-13MYC:natMX6 chk1-9MYC-2HA6his:ura4⁺*	Limbo 2011
OL5086	*h⁻ rad2::kanMX6*	This study
OL4569	*h⁺ rad2::kanMX6*	Williams 2009
OL5087	*h⁻ mre11-W248R-13MYC:kanMX6 pku80::hphMX6*	This study
OL5088	*h⁻ mre11-W248R-13MYC:kanMX6 pku80::hphMX6 exo1::ura4⁺*	This study
OL5089	*h⁻ mre11-W248R-13MYC:kanMX6 exo1::ura4⁺*	This study
OL4176	*h⁻ pku80::hphMX6 exo1::ura4⁺*	Williams 2008
SC4083	*h⁻ pku80::hphMX6*	Williams 2008
OL4175	*h⁻ exo1::ura4⁺*	Williams 2008
OL4564	*h⁻ nbs1-5FLAG:kanMX6*	Williams 2009
OL5090	*h⁺ nbs1-5FLAG:kanMX6*	This study
OL5091	*h⁺ mre11-13MYC:kanMX6 nbs1-5FLAG:kanMX6*	This study
OL5092	*h⁺ mre11-N122S-13MYC:natMX6 nbs1-5FLAG:kanMX6*	This study

OL5093	*h+ mre11-W215C-13MYC:natMX6 nbs1-5FLAG:kanMX6*	This study
OL5094	*h+ TAP-rad50:kanMX6*	This study
OL5095	*h+ TAP-rad50:kanMX6 mre11-13MYC:kanMX6*	This study
OL5096	*h+ mre11-N122S-13MYC:natMX6 TAP-rad50:kanMX6*	This study
OL5097	*h+ mre11-W215C-13MYC:natMX6 TAP-rad50:kanMX6*	This study
OL5098	*h+ mre11-W248R-13MYC:kanMX6 nbs1-5FLAG:kanMX6*	This study
OL5099	*h+ TAP-rad50:kanMX6 mre11-W248R-13MYC:kanMX6*	This study
OL5100	*h+ mre11-CL454RR CV479RR-13MYC:kanMX6 TAP-rad50:kanMX6*	This study
OL4849	*h- rad3::kanMX4 chk1-9MYC-2HA6his:ura4+*	Limbo 2011
OL4877	*h- tel1::hphMX6 chk1-9MYC-2HA6his:ura4+*	Limbo 2011
OL4878	*h- rad3::kanMX4 tel1::hphMX6 chk1-9MYC-2HA6his:ura4+*	Limbo 2011
OL4872	*h- mre11::kanMX4 rad3::natMX6 chk1-9MYC-2HA6his:ura4+*	Limbo 2011
OL5101	*h- mre11-W248R-13MYC:kanMX6 rad3::kanMX4 chk1-9MYC-2HA6his:ura4+*	This study
OL4876	*h+ mre11-H134S-13MYC:kanMX6 rad3::kanMX4 chk1-9MYC-2HA6his:ura4+*	Limbo 2011
YY4139	*h+ ctp1-TAP:hphMX6 arg3::HOsite:kanMX4 ars1:nmt41-HO endonuclease:ampR:his3+:ars1+ his3-D1*	Limbo 2007
OL5116	*h+ ctp1-TAP:hphMX6 mre11-W248R-13MYC:kanMX6 arg3::HOsite:kanMX4 ars1:nmt41-HO endonuclease:ampR:his3+:ars1+ his3?*	This study
OL5103	*h+ nbs1-K522A-5FLAG:kanMX6*	This study
OL5104	*h+ nbs1-K522D-5FLAG:kanMX6*	This study
OL5105	*h+ nbs1-K522E-5FLAG:kanMX6*	This study
OL5106	*h+ nbs1-K522A-5FLAG:kanMX6 mre11-13MYC:kanMX6*	This study
OL5107	*h- nbs1::hphMX6*	This study

Figure S1

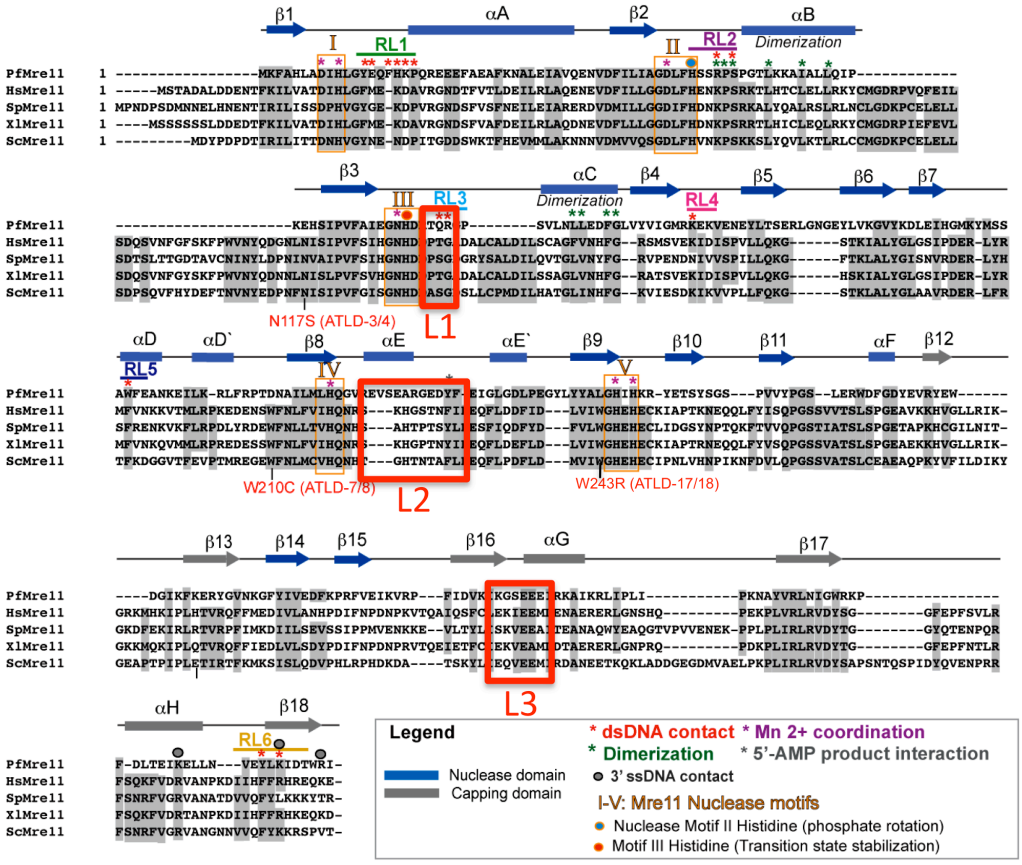

Supplementary Figure S1. Structure-based alignment of Mre11 from *Pyrococcus furiosus* (Pf), *Homo sapiens* (Hs), *Schizosaccharomyces pombe* (Sp), *Xenopus laevis* (Xs), and *Saccharomyces cerevisiae* (Sc). Loop L1 (residues Thr88-Arg90) maps near the dimerization site. This loop, previously referred to as RL3, is predicted to play an important role in the recognition and sculpting of duplex DNA, particularly the 3' strand (8). This loop is not conserved in eukaryotic Mre11, where conserved adjacent Arg and Lys residues are believed to substitute for the RL3 contacts. Loop L2 (Glu178-Phe188) is adjacent to the active site. Loop 3 L3 (Lys279-Glu284) maps to the same central helix of the cap domain that is deleted in the g.2499 G>A allele of ATLD17/18 patients and forms an interface with Rad50 in the open conformation (35).

Figure S2

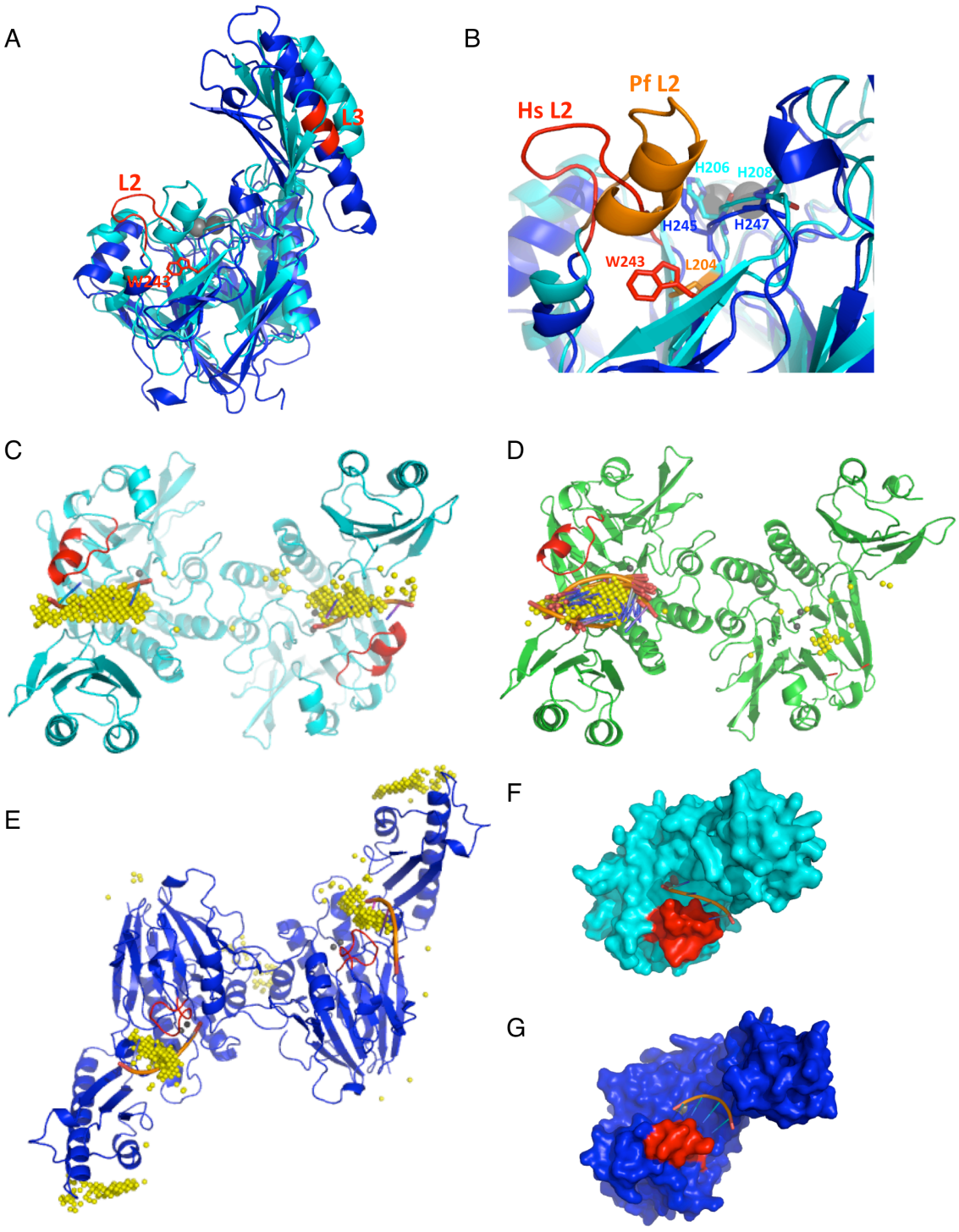

Supplementary Figure S2. Implications of misfolded surface loops DNA binding. (A) Superimposition of HsMre11 (blue) with wild type PfMre11 (cyan) defining regions in the human protein corresponding to L2 and L3 (red). Central helix αF in the cap domain is markedly larger in HsMre11 than its *Pyrococcus* counterpart. (B) Detailed view of

corresponding loops L2 on HsMre11 (red) and wild type PfMre11 (orange). In human Mre11, L2 does not form a structured helix and extends away from cap domain compared to PfMre11. However, a more compact angle between the cap and nuclease domains in HsMre11 in comparison to PfMre11 (76° vs 95°) (33) may compensate for the difference. L2 plays a large role in the formation of a positively charged, L-shaped groove between the nuclease and cap domain of Mre11 that previous computational DNA docking studies suggested in both ssDNA and dsDNA binding (8,26). (C) *In silico* docking (DOT) of a 4 nucleotide ssDNA fragment to the structure of wild type PfMre11 dimer structure (PDB: 1II7). The geometric centers of the ssDNA fragment shown (yellow spheres) represent the top-scoring 2000 solutions, which cluster to the L-shaped grooves in both subunits of wild type PfMre11. (D) DOT docking results for ssDNA performed on PfMre11-L204R dimer structure with L2 removed. DNA still binds to the dimer, but with the great majority clustering to the monomer with the intact L2. (E) DOT docking results for ssDNA on HsMre11 dimer structure (PDB: 3T1I). Clustering of high scoring solutions also occurs in the cap/nuclease groove created by L2 and also in the top of the cap domains, which have been implicated in DNA binding specificity and DNA duplex melting (8). Surface structure of PfMre11 (F) and HsMre11 (G) monomers with modeled DNA of top-scoring solution in nuclease/cap domain interface.

Figure S3

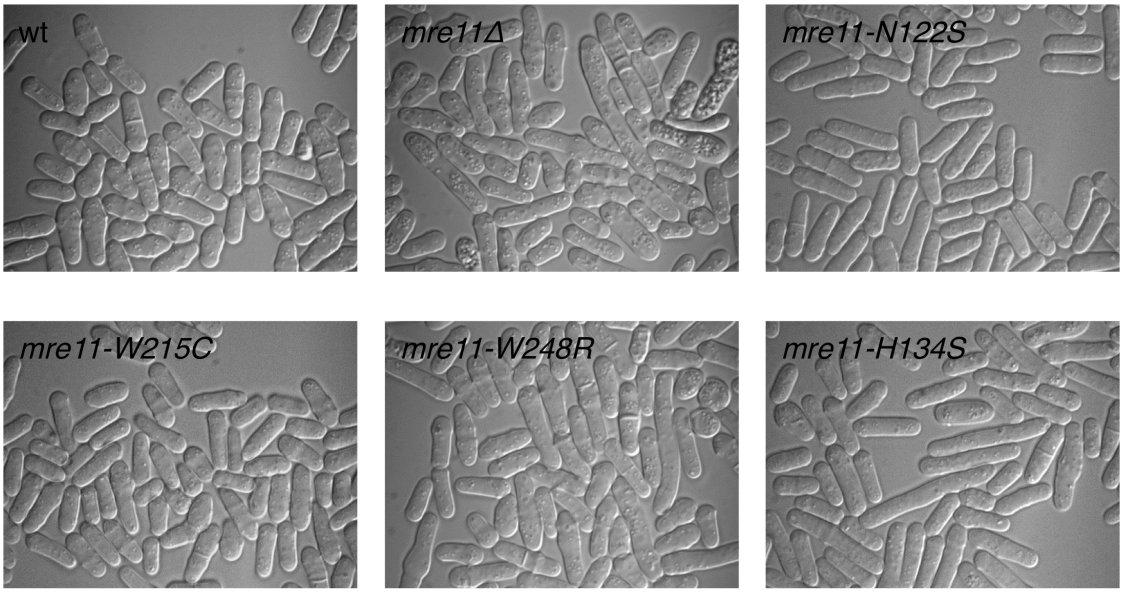

Supplementary Figure S3. Morphology of log-phase *S. pombe* cells with indicated genotype

Figure S4

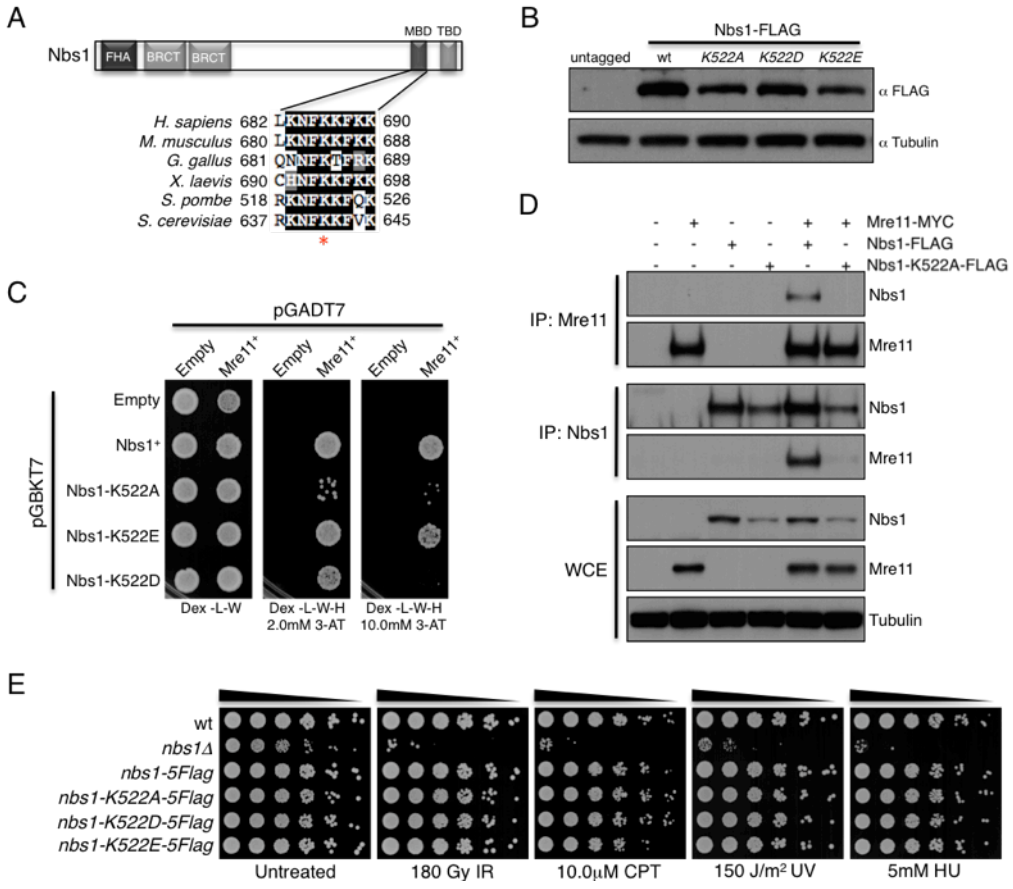

Supplementary Figure S4. Mutation of Mre11 binding domain in Nbs1. (A) Nbs1 domain architecture and local alignment of Mre11 binding domain (MBD). * denotes mutated lysine residue. TBD = Tel1^{ATM} binding domain. (B) Nbs1 protein expression levels. Tubulin shows loading. (C) Pair-wise yeast-2-hybrid with reporter strain AH109 co-transformed with indicated cDNAs fused to activating domain (pGADT7) or DNA binding domain (pGBKT7) of Gal4 transcription factor. Positive co-transformants selected on dextrose dropout media lacking tryptophan(W) and leucine(L). Positive interactions were assayed by growth on dextrose dropout media lacking tryptophan(W), leucine(L), and histidine(H) with indicated dose of *HIS3* (reporter gene) competitive inhibitor, 3-AT. (D) Reciprocal co-immunoprecipitation of Nbs1 and Mre11. Proteins were precipitated and detected using FLAG, MYC, or tubulin antibodies fused to Nbs1 and Mre11. (E) DNA damage sensitivity assay of Nbs1 mutants.

SUPPLEMENTARY MATERIALS AND METHODS

Human Mre11 expression and purification

Human Mre11 WT and MRE11 W243R preparations were produced by infection of Sf9 cells in suspension culture with baculoviruses expressing C-terminally 6-histidine tagged human MRE11 WT or MRE11 W243R. Cells were collected after 72 hours, washed two times in PBS and frozen in liquid nitrogen. Cells were thawed and resuspended in four packed cell volumes of ice cold buffer A (50 mM Tris-HCl pH 8.0, 500 mM NaCl, 2mM β-mercaptoethanol, 5% glycerol and 1 complete, EDTA-free Protease inhibitor cocktail tablet from Roche). The cells were disrupted by 20 strokes of a type B pestle in a Dounce homogenizer. After 1 hour of centrifugation at 35K (Beckman, rotor 45 Ti) at 4°C, the soluble fraction was incubated overnight at 4°C with half packed cell volume of Ni^{2+}-NTA agarosebeads (Qiagen), equilibrated in buffer A containing 5 mM imidazole. The column, containing beads, was washed with 10 volumes of buffer A containing 5 mM imidazole. Additionally the column was washed with 3 volumes of buffer A containing 40 mM imidazole. Bound proteins were eluted from the beads in buffer B(50 mM Tris-HCl pH 8.0, 300 mM NaCl, 2mM β-mercaptoethanol, 5% glycerol and 200mM imidazole). The MRE11 containing fractions were pooled and loaded on a Superdex 200 size-exclusion column (GE Healthcare) that was equilibrated in buffer C (50 mM Tris-HCl pH 8.0, 200 mM NaCl, 1 mM DTT). The MRE11 containing fractions were pooled and diluted before being loaded onto a 5 mL Hitrap Q column. The column was washed with ten column volumes of buffer D(50 mM Tris-HCl pH 8.0 and 1 mM DTT) containing 100mM NaCl, three column volumes of buffer D containing 200 mM. The proteins were eluted from the column in buffer D using a linear gradient of 200mM – 1 M NaCl, in five column volumes. The fractions containing MRE11 were pooled and concentrated on a 1 mL Heparin column. The column was washed with 28 column volumes of buffer D containing 100mM NaCl and 10% glycerol. MRE11 was eluted in buffer D containing 10% glycerol using a gradient of 200mM – 500 mM NaCl. MRE11 containing fractions were pooled, aliquoted and frozen in liquid nitrogen. Immuno-blotting of MRE11 was performed on nitrocellulose transfer membrane (Whatman) using standard immuno-blotting techniques. Protein concentrations were determined by comparison to a BSA standard on a 10 % polyacrylamide gel after staining with Coomassie blue.

DNA Docking (DOT)

Docking calculations were performed with the program DOT (www.sdsc.edu/CCMS) (66-68) using a linear 4 nucleotide (5'-TTTT-3') B-DNA fragment generated using X3DNA program moved within the shape and electrostatic potentials of stationary Mre11 structures. The distribution of the top-ranked 2000 geometric centers of the DNA fragments was analyzed for number and distribution over the Mre11 protein structure (represented as yellow spheres). Of these, the top solution was used to determine the orientation of the DNA.

Rigid-body docking of DNA to the Mre11 protein requires addition of polar hydrogen atoms to the Mre11 X-ray coordinates extracted from PDB. All hydrogen atoms were added to the Mre11 coordinates with the program REDUCE using the –build

option. REDUCE also determined the preferred orientations for Asn, Gln, and His side chains and His protonation states based on the local environment.

One molecule represented by its atomic positions with partial atomic charges (DNA), is systematically moved within the shape and electrostatic potentials of a stationary molecule (Mre11 structure). Interaction energies, calculated as the sum of electrostatics and Van der Waals terms, are evaluated as correlation functions, which are efficiently computed with Fast Fourier Transforms. The properties of both molecules, calculated by an automated set-up procedure in the DOT2 suite, were mapped onto cubic grids 128 Å on a side with 1 Å grid spacing. This grid size was sufficiently large to ensure that the DNA coordinates fit within the grid when the DNA was close to Mre11, and that artifacts from the periodic Fourier calculation were negligible. A set of 54,000 orientations was used for the DNA, providing a rotational search approximately as fine as the 1 Å translational search. Each orientation of the DNA was centered at all grid points in a highly efficient translational search, giving about 108 billion configurations of the two molecules. Each docking calculation took around 1 h on 8 processors at Garibaldi cluster at The Scripps Research Institute.

EMSAs

ssDNA90 5'-AAT TCT CAT TTT ACT TAC CGG ACG CTA TTA GCA GTG GCA GAT TGT ACT GAG AGT GCA CCA TAT GCG GTG TGA AAT ACC GCA CAG ATG CGT- 3' from Eurogentec

dsDNA90 5'-AAT TCT CAT TTT ACT TAC CGG ACG CTA TTA GCA GTG GCA GAT TGT ACT GAG AGT GCA CCA TAT GCG GTG TGA AAT ACC GCA CAG ATG CGT- 3' annealed to its complementary oligo 5'- ACG CAT CTG TGC GGT ATT TCA CAC CGC ATA TGG TGC ACT CTC AGT ACA ATC TGC CAC TGC TAA TAG CGT CCG GTA AGT AAA ATG AGA ATT-3' from Eurogentec

Binding buffer: 5% glycerol, 25mM Tris-HCl pH 7.5, 100mM NaCl, 1mM DTT and 2% PEG6000 for 10 min at 25°C in a final volume of 20µL for human Mre11 and 5% glycerol, 25mM HEPES pH 8.0, 50mM NaCl, 1 mM DTT, and 2% PEG6000 for 20 min at 45°C in a final volume of 20µL for *P. furiosus* Mre11.

Nuclease Assays

2µg of purified *Pf*Mre11 (WT or L204R) and 1.5 µg of ϕX174 circular ssDNA Virion DNA (New England Biolabs) in a 12µl volume of 25mM HEPES pH 7.0, 25mM NaCl, and 5mM $MnCl_2$ were incubated at 50°C at the indicated time points. Reactions were stopped by the addition of EDTA to a final concentration of 20mM and 2.5mg/ml proteinase K. DNA was resolved by electrophoresis in 1% TAE agarose gels.

One hundred nanograms of PhiX174 circular single-stranded virion DNA substrate (5386 bases, New England Biolabs) was incubated with three hundred nanograms of hMRE11 WT or hMRE11W243R in reaction buffer (30mM Tris-HCl pH 7.5, 1mM dithiothreitol, 25mM KCl, 200ng acetylated bovine serum albumin and 5mM of either $MgCl_2$ or $MnCl_2$) for the indicated times at 37°C in a 20-µl reaction mixture. The nuclease reactions were terminated by incubation for 10 minutes at 37°C after the addition of 1/10 volume of stop solution (3% SDS, 50mM EDTA) and proteinase K to a final concentration of 0.1 mg/ml. The reaction products were run in a 0.8% agarose gel (1xTAE) for 90 minutes at 100mA. DNA was stained by Ethidiumbromide and

visualized by scanning of the gel using a image analyzer (Typhoon9200). Quantification was performed with ImageQuant 5.2 software.

Fifty nanograms of linear blunt-ended double-stranded DNA (pBluescript, 2961bp) was incubated with five hundred nanograms of hMRE11 WT or hMRE11W243R in reactionbuffer (30mM Tris-HCl pH 7.5, 1mM dithiothreitol, 25mM KCl, 200ng acetylated bovine serum albumin and 5mM of either $MgCl_2$ or $MnCl_2$) for the indicated times at 37°C in a 20-µl reaction mixture. The nuclease reactions were terminated by incubation for 20 minutes at 37°C and 10 minutes at 85°C after the addition of 1/10 volume of stop solution (3% SDS, 50mM EDTA) and proteinase K to a final concentration of 1 mg/ml. The reaction products were run in a 1.5% agarose gel (1xTAE) for 240 minutes at 100mA. DNA was stained by Ethidiumbromide and visualized by scanning of the gel using an image analyzer (Typhoon9200). Quantification was performed with ImageQuant 5.2 software Quantification of the data was performed with ImageQuant 5.2 software.

Telomere Southern blot

Genomic DNA was isolated and resolved as described previously (28). DNA was transferred to Biodyne B membrane (Pall Life Sciences) via capillary transfer and crosslinked by UV irradiation. The membrane was washed 20 minutes in 5X SSPE buffer and pre-hybridized with Denhardts solution with sheared/denatured salmon sperm DNA for 1 hour at 65°C. The probe was generated by PCR amplification of the TAS1 sequence from plasmid pNSU70 (31) using the following primers:

5’ – CCA ATA GTG GGG GCA TTG TAT TTG – 3’
5’ – CAC TAA TTG TAA TAA GGT GG – 3’

incorporating 85% biotinylated dCTP (TriLink N-5002) and 15% normal dCTP. The probe was gel purified, denatured, and added to the pre-hybridization solution and incubated with the membrane overnight at 65°C. The membrane was washed 3 times in 2X SSPE for 15 minutes at 65°C, blocked with Odyssey blocking solution with 1% SDS for 1 hour at room temperature, and incubated with IRdye 680 conjugated strepavidin (Li-Cor 926-68031) at 1:10,000 for 1 hour at room temperature. The membrane was washed 3 times in PBS with 0.1% Tween-20 for 5 minutes and once for 5 minutes in PBS. Membrane was scanned with Li-Cor Odyssey Infrared Imaging System at intensity 7. Image shown is representative of 3 independent experiments.

SUPPLEMENTARY REFERENCES

5. Williams, R.S., Dodson, G.E., Limbo, O., Yamada, Y., Williams, J.S., Guenther, G., Classen, S., Glover, J.N., Iwasaki, H., Russell, P. *et al.* (2009) Nbs1 flexibly tethers Ctp1 and Mre11-Rad50 to coordinate DNA double-strand break processing and repair. *Cell*, **139**, 87-99.

8. Williams, R.S., Moncalian, G., Williams, J.S., Yamada, Y., Limbo, O., Shin, D.S., Groocock, L.M., Cahill, D., Hitomi, C., Guenther, G. *et al.* (2008) Mre11 dimers coordinate DNA end bridging and nuclease processing in double-strand-break repair. *Cell*, **135**, 97-109.

26. Hopfner, K.P., Karcher, A., Craig, L., Woo, T.T., Carney, J.P. and Tainer, J.A. (2001) Structural biochemistry and interaction architecture of the DNA double-strand break repair Mre11 nuclease and Rad50-ATPase. *Cell*, **105**, 473-485.

28. Limbo, O., Chahwan, C., Yamada, Y., de Bruin, R.A., Wittenberg, C. and Russell, P. (2007) Ctp1 is a cell-cycle-regulated protein that functions with Mre11 complex to control double-strand break repair by homologous recombination. *Mol Cell*, **28**, 134-146.

30. Limbo, O., Porter-Goff, M.E., Rhind, N. and Russell, P. (2011) Mre11 nuclease activity and Ctp1 regulate Chk1 activation by Rad3ATR and Tel1ATM checkpoint kinases at double-strand breaks. *Mol Cell Biol*, **31**, 573-583.

31. Nakamura, T.M., Cooper, J.P. and Cech, T.R. (1998) Two modes of survival of fission yeast without telomerase. *Science*, **282**, 493-496.

33. Park, Y.B., Chae, J., Kim, Y.C. and Cho, Y. (2011) Crystal structure of human Mre11: understanding tumorigenic mutations. *Structure*, **19**, 1591-1602.

35. Mockel, C., Lammens, K., Schele, A. and Hopfner, K.P. (2011) ATP driven structural changes of the bacterial Mre11:Rad50 catalytic head complex. *Nucleic Acids Res*.

36. Porter-Goff, M.E. and Rhind, N. (2009) The role of MRN in the S-phase DNA damage checkpoint is independent of its Ctp1-dependent roles in double-strand break repair and checkpoint signaling. *Mol Biol Cell*, **20**, 2096-2107.

65. Du, L.L., Moser, B.A. and Russell, P. (2004) Homo-oligomerization is the essential function of the tandem BRCT domains in the checkpoint protein Crb2. *J Biol Chem*, **279**, 38409-38414.

66. Mandell, J.G., Roberts, V.A., Pique, M.E., Kotlovyi, V., Mitchell, J.C., Nelson, E., Tsigelny, I. and Ten Eyck, L.F. (2001) Protein docking using continuum electrostatics and geometric fit. *Protein Eng*, **14**, 105-113.

67. Roberts, V.A. and Pique, M.E. (1999) Definition of the interaction domain for cytochrome c on cytochrome c oxidase. III. Prediction of the docked complex by a complete, systematic search. *J Biol Chem*, **274**, 38051-38060.

68. Roberts, V.A., Pique, M.E., Hsu, S., Li, S., Slupphaug, G., Rambo, R.P., Jamison, J.W., Liu, T., Lee, J.H., Tainer, J.A. *et al.* (2012) Combining H/D exchange mass spectroscopy and computational docking reveals extended DNA-binding surface on uracil-DNA glycosylase. *Nucleic Acids Res*, **40**, 6070-6081.